# STAT6-Dependent Exacerbation of House Dust Mite-Induced Allergic Airway Disease in Mice by Multi-Walled Carbon Nanotubes

**Mark D. Ihrie**[a], **Katherine S. Duke**[a], **Kelly A. Shipkowski**[a], **Dorothy J. You**[a], **Ho Young Lee**[a], **Alexia J. Taylor-Just**[a], **James C. Bonner**[a,*]

[a]Toxicology Program, Department of Biological Sciences, North Carolina State University, Raleigh, North Carolina 27695 U.S.A

## Abstract

There is increasing evidence that inhaled multi-walled carbon nanotubes (MWCNTs) can have harmful effects on the respiratory system. Rodent studies suggest that individuals with asthma may be susceptible to the adverse pulmonary effects of MWCNTs. Asthma is an allergic lung disease characterized by a $T_H2$ immune response that results in chronic airway disease characterized by eosinophilic lung inflammation, airway mucous cell metaplasia, and airway fibrosis. Signal transducer and activator of transcription 6 (STAT6) is a transcription factor with multiple roles in $T_H2$ type inflammation. Herein we sought to examine the role of STAT6 in the exacerbation of house dust mite (HDM) allergen-induced allergic airway disease by MWCNTs. Male wild type (WT) and STAT6 knockout (*Stat6* KO) mice were dosed via intranasal aspiration on days 0, 2, 4, 14, 16 and 18 with either vehicle, HDM extract, MWCNTs, or a combination of HDM and MWCNTs. Necropsy was performed on day 21 to collect bronchoalveolar lavage fluid (BALF), serum and lung tissue. MWCNTs exacerbated HDM-induced allergic endpoints, including eosinophilic lung inflammation, mucous cell metaplasia, and serum IgE levels. HDM-induced eosinophilic lung inflammation, mucous cell metaplasia, and serum IgE and exacerbation of these endpoints by MWCNTs were ablated in *Stat6* KO mice. In addition, airway fibrosis was significantly increased by the combination of HDM and MWCNTs in WT mice but not in *Stat6* KO mice. These findings provide new mechanistic insight by demonstrating a requirement for STAT6 in MWCNT-induced exacerbation of allergic respiratory disease.

### Keywords

carbon nanotubes; house dust mite; allergens; STAT6; asthma

## 1.  Background

The nanotechnology industry has undergone rapid growth in recent years, resulting in a variety of different types of engineered nanomaterials (ENMs) with diverse applications in medicine, engineering, and electronics (WHO 2020). This growth has been accompanied by an increasing concern over the potential toxic effects of ENMs, and there is now strong evidence from rodent models that inhalation exposure to ENMs can cause lung injury and systemic immunotoxicity (Ihrie and Bonner, 2018). Nanoscale materials are defined as having at least one dimension less than 100 nm, and include fiber-like ENMs such as multi-walled carbon nanotubes (MWCNTs) (Donaldson et al., 2006). MWCNTs, typically 10-100 nm in diameter and microns in length, have been of particular concern due to their fiber-like structure and small size, which allows them to deposit and persist in the distal region of the lung to cause injury, inflammation, and fibrosis (Donaldson et al., 2006).

Studies in mice have shown that pulmonary exposure to MWCNTs can cause fibrosis, altered immune responses, and exacerbation of allergic endpoints (Duke and Bonner, 2018; Ihrie and Bonner, 2018). It is also important to consider that the toxicity of different types of MWCNTs can vary greatly, as the pulmonary immune response to MWCNTs depends on their physicochemical characteristics, including size, surface coating and rigidity (Duke et al., 2017; Rydman et al., 2014). While exposure to MWCNTs alone can result in pathological outcomes, pre-exposure or post-exposure to MWCNTs has been shown to exacerbate allergen-induced lung disease (Ihrie et al., 2019; Inoue et al., 2009; Nygaard et al., 2009; Ronzani et al., 2014; Ryman-Rasmussen et al., 2009; Shipkowski et al., 2015).

Asthma is a chronic inflammatory airway disease characterized by airway hyperresponsiveness, eosinophilic inflammation, mucous cell metaplasia, and airway fibrosis (Holgate, 2009; Ozdoganoglu and Songu, 2012). Together these characteristics lead to airway obstruction and impaired lung function (Holgate, 2009). Asthma results from innate and adaptive immune responses to environmental allergens from agents such as mold, pollen, cockroaches, and house dust mites (Kim et al., 2010). In the classic paradigm of allergic asthma, sensitization occurs when inhaled environmental allergens are taken up and processed by antigen presenting cells in the lung (e.g., dendritic cells and macrophages), which subsequently present the antigen to naïve helper T cells to initiate $T_H2$ cell polarization (Holgate, 2009; Kim et al., 2010). This $T_H2$ environment is characterized by interleukin (IL)-4 and IL-13 production, as well as antigen-specific immunoglobulin E (IgE) production by B cells. Innate immune cells also play important roles in the pathogenesis of asthma; allergic asthma is generally eosinophilic, although exacerbation by factors such as ozone, cigarette smoke, or air pollution particulates can result in mixed eosinophilic and neutrophilic inflammation (Holgate, 2009). A variety of other lung cells also play vital roles in asthma. For example, epithelial cells undergo mucous cell metaplasia in response to the cytokine environment and over-produce mucus, while sub-epithelial fibroblasts surrounding

the airways produce collagen causing fibrosis, contributing to airway wall remodeling in chronic asthma (Holgate, 2009).

The signal transducer and activator of transcription (STAT) family of transcription factors consists of seven members that reside in the cytoplasm, awaiting activation by upstream signals (Hebenstreit et al., 2006; Rawlings et al., 2004). In brief, the STAT signal cascade consists of the ligand binding to its receptor followed by homo or heterodimerization. Each receptor subunit is associated with a JAK tyrosine kinase, which upon dimerization undergo trans-phosphorylation (Hebenstreit et al., 2006; Rawlings et al., 2004). The activated JAKs then phosphorylate both the receptor and the cytoplasmic STATs. Phosphorylated STATs dimerize and translocate to the nucleus where they bind specific gene sequences to activate target genes. STAT6 mediates the biological effects of $T_H2$ cytokines (IL-4 and IL-13) and thereby plays an important role in the pathogenesis of asthma (Walford and Doherty, 2013). STAT6 is expressed in many different immune cell types involved in allergic lung inflammation, and plays key roles in each of these cell types (Chapoval et al., 2011). For example, STAT6 mediates Ig ε chain expression in B cells upon exposure to IL-4 or IL-13, causing Ig isotype switching and IgE production. In T cells, *Gata3* expression is induced via STAT6 which leads to $T_H2$ polarization (Walford and Doherty, 2013). In airway epithelial cells, STAT6 mediates the induction of mucin genes such as *Muc5ac* by IL-4 or IL-13, leading to mucous cell metaplasia. STAT6 also regulates airway smooth muscle contractility and macrophage polarization. *Stat6* knockout (KO) mice do not develop most of the phenotypes associated with allergic airway disease, including eosinophilic lung inflammation, mucous cell metaplasia, or airway hyperresponsivity to allergens (Akimoto et al., 1998; Kuperman et al., 1998). However, the role of STAT6 in the exacerbation of allergic airway disease by environmental factors, including ambient or engineered nanoparticles, is unknown.

Mouse models of asthma or allergic lung disease are achieved by repeated sensitization and challenge to allergens such as ovalbumin (OVA), or from environmentally relevant allergens such as those derived from house dust mites (HDM), including Der p1 and Der p2 (Castañeda and Pinkerton, 2016). We previously reported that MWCNT exposure exacerbates either OVA- or HDM-induced allergen-induced airway fibrosis in mice (Ryman-Rasmussen et al., 2009; Shipkowski et al., 2015). Moreover, we reported that *Stat1* KO mice were susceptible to exacerbation of OVA-induced airway disease by MWCNTs, demonstrating that STAT1 plays a protective role that counteracts the allergic inflammatory responses mediated by STAT6 (Thompson et al., 2015). *Stat6* KO mice display attenuated lung fibrosis upon oropharyngeal aspiration of rod-like (Mitsui-7) MWCNTs in the absence of any allergen (Nikota et al., 2017). However, Mitsui-7 MWCNTs are not representative of most commercially available MWCNTs, which have a tangled morphology, and alone do not directly activate STAT6, but rather exacerbate allergen-induced $T_H2$ immune responses (Shipkowski et al., 2015; Duke et al., 2017; Ihrie et al., 2019). It is unknown whether STAT6 mediates exacerbation of allergen-induced lung disease in mice by MWCNTs or any other type of ENM. Therefore, we sought to examine the requirement of STAT6 in the exacerbation of HDM-induced allergic airway disease by tangled MWCNTs using an intranasal aspiration co-exposure protocol comparing WT and *Stat6* KO mice. We observed that MWCNTs significantly exacerbated HDM-induced allergic endpoints in WT mice,

including eosinophilic lung inflammation, serum IgE levels, and mucous cell metaplasia, while allergen induction of these endpoints and exacerbation by MWCNTs in *Stat6* KO mice was greatly reduced. In addition, airway fibrosis was significantly increased by the combination of HDM and MWCNTs in WT mice but not in *Stat6* KO mice. These findings demonstrate a requirement for STAT6 in MWCNT-induced exacerbation of allergic respiratory disease.

## 2. Methods

### 2.1. Nanomaterials and House Dust Mite Allergen

MWCNTs were purchased from Helix Material Solutions Inc. (Richardson, TX) and suspended in 0.1% Pluronic in DPBS at a stock concentration of 10 mg/ml and sonicated in a cup horn sonicator for 3 minutes. These MWCNTs have been previously used in studies of exacerbation of OVA allergen-induced lung disease in transgenic mice (Sayers et al., 2013; Thompson et al., 2015). The physicochemical characteristics of these MWCNTs have been previously reported (Ryman-Rasmussen et al., 2009). Moreover, we have also reported suspension characteristics of these MWCNTs in aqueous media using dynamic light scattering (Taylor et al., 2014). Briefly, the length ranged from 0.5 to 40 μm as determined by scanning electron microscopy (SEM), the average diameter ranged from 10 to 30 nm as determined by transmission electron microscopy (TEM), and residual nickel content was 5.53 + 3.92% as determined by energy-dispersive X-ray spectroscopy (EDX). HDM extract was purchased from Greer Laboratories Inc. (Lenoir, NC). Lyophilized HDM was dissolved in 0.1% Pluronic in DPBS at a stock concentration of 1 mg/ml. The HDM extract contained 927.5 endotoxin units (EU), determined by amoebocyte lysate test, according to the manufacturer. This HDM extract was partially characterized by proteomic analysis using LC-MS/MS at NCSU, which qualitatively identified a variety of proteases including alpha-amylase, cysteine proteinase-1, serine protease LM-1, trypsin-like serine protease, Der p 1, Der p 2, Der p 3, Der p 13, and Der p 20 (unpublished data).

### 2.2. Animals and Experimental Design

Pathogen free 8 to 10-week old male C57BL/6 (WT) mice and *Stat6* KO mice were purchased from Jackson Laboratories (Bar Harbor, ME). Animals were housed in an AALAC-accredited animal facility at NCSU. All procedures were approved by the NCSU Institutional Animal Care and Use Committee. Animals were acclimated for two weeks prior to dosing, housed 5 per cage and provided water and LabDiet 5001 rodent diet *ad libitum.* MWCNTs and HDM were prepared at working concentrations of 0.25 mg/ml and 0.5 mg/ml, respectively, in 0.1% Pluronic in DPBS. Mice were anesthetized with isoflurane and dosed with 50 μl of vehicle (0.1% Pluronic in DPBS), HDM, MWCNTs, or HDM and MWCNTs by intranasal aspiration (25 μg of HDM and 12.5 μg of MWCNTs per dose). As illustrated in Fig. 1, mice were dosed 3 times in the first week (days 0, 2, and 4) and 3 times in the third week (days 14, 16, and 18) and were euthanized by an intraperitoneal injection of pentobarbital (Fatal Plus, Vortech Pharmaceuticals, Dearborn, MI) 3 days after the last dose (day 21). The 6 doses yielded a total MWCNT dose of 75 μg, approximately 3 mg/kg, and total HDM dose of 150 μg. Treatment groups consisted of 4-6 mice.

### 2.3. Necropsy and Tissue Collection

Bronchoalveolar lavage fluid (BALF) was collected by lavaging the lungs twice with 0.5 ml sterile DPBS via intratracheal cannulation. A Thermo Scientific Cytospin 4 Cytocentrifuge (Thermo Fisher Scientific, Waltham, MA) was used to isolate cells from 100 μl of BALF onto glass slides. Cells were then fixed and stained with the Diff-Quik Stain Set (Siemens, Newark, DE). The remaining BALF was stored at −80° C. After BALF collection, the middle and caudal lobes of the right lung were placed in RNAlater (Ambion, Austin, TX), according to the manufacturer's instructions and stored at −80° C. The cranial lobe of the right lung was flash frozen in liquid nitrogen and stored at −80° C. The left lung was infused with 10% neutral buffered formalin, fixed for 24 hours, dehydrated stepwise in 70% ethanol and then 100% ethanol, and embedded in paraffin. Whole blood was collected from the jugular veins, allowed to coagulate for 15 minutes in Serum Separator Tubes (BD Microtainer, Franklin Lakes, NJ), then centrifuged to obtain serum. Serum was stored at −80° C.

**ELISA.**—DuoSet ELISA kits (R&D Systems, Inc.) were used to measure total IgE in serum and interleukin (IL)-1β, IL-13, transforming growth factor (TGF)-β1, and osteopontin (OPN) in BALF. Serum was diluted 1:10 in DPBS for the IgE ELISA. ELISAs were carried out according to the manufacturer's protocol.

### 2.4. Cell Counting and Histology

For evaluation of lung inflammatory cells, 100 μl of BALF was centrifuged using a Cytospin 4 centrifuge (ThermoFisher, Waltham, MA) to isolate cells on glass slides. The slides were then fixed and stained with the Diff-Quik stain set (Siemens, Newark, DE). The average count of all cell types was quantified by using an Olympus light microscope BX41 (Center Valley, PA) according to a previously published method (Shipkowski et al., 2015). Three representative photomicrographs were taken per animal at 100x magnification, and every cell type counted using ImageJ software with Fiji expansion [Eliceiri/LOCI group, University of Wisconsin-Madison, Madison, WI). Cell differentials were quantified by counting 500 cells per slide/animal to determine relative numbers of macrophages, neutrophils, eosinophils and lymphocytes. Paraffin embedded tissues were cut into three sections and stained with hematoxylin and eosin (H&E), Alcian blue/periodic acid-Schiff (AB/PAS) and/or Gomori trichrome stain.

### 2.5. Semi-Quantitative Morphometric Analysis

Mucous cell metaplasia and airway mucus production was assessed by imaging all airways under approximately 500x500 μm (HxW) in each AB/PAS-stained sample and quantifying the area of positive staining in ImageJ (National Institutes of Health) as percent area. Airway fibrosis was assessed by imaging Gomori's trichrome stained lung sections and obtaining area to perimeter ratios as described previously (Duke et al., 2017). Briefly, round to oval shaped airways under 500x500 μm (HxW) were imaged at 100x. The lasso tool in Adobe Photoshop CS5 was used to surround trichrome positive collagen around the airways, giving the outer area, and to surround the basement membrane, giving the inner area and circumference (perimeter). The difference between the outer and inner area was divided by

the circumference giving the area/perimeter ratio. All measurements were performed in a blinded manner.

### 2.6. Western Blotting

Protein concentrations from snap-frozen lung tissue was determined using the Pierce BCA Protein Assay Kit (ThermoFisher Scientific, Waltham, MA). Samples were diluted, loaded on a Novex™ 4–12% Tris-Glycine Mini Gel (Invitrogen, Carlsbad, CA) and separated by electrophoresis. Separated proteins were transferred to a PVDF membrane, blocked, and incubated in primary antibody at a 1000x dilution. Rabbit polyclonal STAT1, STAT3, STAT6 and β-actin primary antibodies and anti-rabbit secondary antibody were purchased from Cell Signaling Technology (Beverly, MA). After incubation with primary antibody, membranes were washed and incubated in secondary antibody at a 2500x dilution. Enhanced chemiluminescent reagent (ThermoFisher Scientific) was used to visualize antibody signals. Densitometry was performed to quantify western blot signals. Briefly, high resolution scans were analyzed in Adobe Photoshop CS5 by setting the white point to the background, inverting the image, and measuring the mean grey value of each band. For phosphorylated STAT proteins, this value was divided by the total STAT protein value.

### 2.7. Statistical Analysis

All data were graphed and analyzed using GraphPad Prism version 5 (GraphPad Software Inc., San Diego, CA). Significance between treatment groups was determined by two-way ANOVA with a Tukey's post-test, Student's t-test, or Mann Whitney test. All data are represented as the mean + SEM of four to six animal replicates.

## 3. Results

### 3.1. Alveolar macrophage uptake of MWCNTs delivered by intranasal aspiration

TEM images of bulk MWCNTs that were used in this study are shown in Fig. 1A. MWCNTs, with or without HDM extract, were delivered by intranasal aspiration according the protocol illustrated in Fig. 1B. This protocol resulted in the delivery of well-dispersed MWCNTs to the distal airways and alveoli where they were taken up by alveolar macrophages. Macrophages isolated from the lungs of mice by bronchoalveolar lavage post-exposure contained MWCNTs within their cytoplasm (Fig. 1C). Moreover, MWCNTs were observed within the macrophages in the alveolar region *in situ* (Fig. 1D).

### 3.2. STAT6-dependent enhancement of HDM-induced eosinophilic lung inflammation by MWCNTs

Microscopic images of BALF cells fixed to glass slides by Cytospin centrifugation showed that MWCNTs enhanced HDM-induced cellularity in the lungs of WT mice (Fig. 2A). Quantification of total cell counts and differential cell counts showed that the increase in cellularity in the BALF of WT mice exposed to HDM or combined HDM and MWCNTs was due to eosinophils. However, significantly greater numbers of lymphocytes were observed in the BALF of *Stat6* KO mice compared to WT mice (Fig. 2B–F).

### 3.3. STAT6-dependent mucous cell metaplasia by HDM and MWCNT co-exposure

AB/PAS staining showed mucosubstances in the airway of WT mice exposed to HDM and treatment of WT mice with a combination of MWCNTs and HDM extract caused enhanced airway mucosubstances compared to HDM treatment alone (Fig. 3A). Virtually no mucosubstances were observed in the lungs of any *Stat6* KO mice exposed to either HDM extract alone or the combination of HDM and MWCNTs (Fig. 3A). Quantification showed that HDM extract alone or HDM and MWCNT co-exposure significantly increased mucin production in WT mice, but not *Stat6* KO mice (Fig. 3B).

### 3.4. STAT6-dependent enhancement of HDM-induced serum IgE by MWCNTs

Serum IgE was synergistically enhanced by exposure to HDM extract and MWCNTs in WT mice, whereas HDM extract or MWCNTs alone did not significantly increase serum IgE levels (Fig. 4). In contrast, *Stat6* KO mice did not display increased serum IgE levels in response to combined HDM extract and MWCNT treatment.

### 3.5. Airway fibrosis induced by HDM and MWCNTs in WT and Stat6 KO mice

Trichrome staining revealed peribronchiolar fibrosis in WT mice exposed to HDM extract and MWCNTs (Fig. 5A). Quantitative morphometry of trichrome-positive lesions assessed by an area/perimeter ratio method revealed a significant increase in airway fibrosis in WT mice exposed to HDM extract and MWCNTs, but not with either HDM extract or MWCNTs alone (Fig. 5B). Moreover, there was no significant increase in airway fibrosis in *Stat6* KO mice.

### 3.6. Cytokines in BALF of WT and Stat6 KO mice after treatment with HDM extract in the absence or presence of MWCNTs

A panel of cytokines (IL-13, IL-1β, TGF-β1, OPN) were measured by ELISA in BALF at 21 days (Fig. 6). IL-13 was suppressed by MWCNTs in the absence or presence of HDM extract in WT but not *Stat6* KO mice. IL-1β was suppressed by MWCNTs in WT mice but increased by HDM extract in *Stat6* KO mice. No significant changes were observed in TGF-β1 or OPN among treatment groups or between genotypes.

### 3.7. STAT1 and STAT3 in lung tissue from WT and Stat6 KO mice after treatment with HDM extract in the absence or presence of MWCNTs

STAT1 and STAT3 proteins were measured by Western blotting in lung lysates collected at 21 days after exposure to HDM with or without MWCNTs (Fig. 7). Representative Western blots are shown in Fig. 7A. As expected, *Stat6* KO mice contained no STAT6 protein in lung tissue. STAT1 protein in lung tissue was significantly higher in untreated WT mice compared to *Stat6* KO mice, but was not significantly altered by exposure to HDM with or without MWCNTs (Fig. 7A and B). Phospho-STAT3 normalized to total STAT3 in lung tissue was increased by co-exposure to HDM and MWCNTs in WT mice compared to vehicle, but not by HDM or MWCNTs alone (Fig. 7C). *Stat6* KO mice coexposed to HDM and MWCNTs also had an elevated pSTAT3/STAT3 ratio, but not to a statistically significant level, and there was no significant difference between WT and Stat6 KO mice co-exposed to

HDM and MWCNTs. Total STAT3 normalized to β-actin was not altered by exposure to HDM and/or MWCNTs (Fig. 7D).

## 4. Discussion

This study demonstrated a requirement for STAT6 in the exacerbation of allergic lung inflammation by MWCNTs, an ENM that is produced in high volume and therefore represents a potential hazard for human exposure. *Stat6* KO mice exhibited loss of phenotypic endpoints of allergic airway disease (eosinophilic lung inflammation, mucous cell metaplasia, IgE production) induced by HDM exposure and exacerbated by MWCNTs. Seminal work over twenty years ago, using *Stat6* KO mice, demonstrated a pivotal role for STAT6 in mediating allergen-induced lung disease in mice (Akimoto et al., 1998; Kuperman et al., 1998). These studies showed that *Stat6* KO mice sensitized and challenged with OVA, compared to WT mice, had fewer numbers of eosinophils in BALF, reduced $T_H2$ cytokines (IL-4 and IL-13) and serum IgE, suppressed mucous cell metaplasia, and reduced airway hyperreactivity (AHR). Similarly, we observed that *Stat6* KO mice had fewer numbers of eosinophils in BALF, reduced serum IgE and loss of airway mucous cell metaplasia in response to HDM allergen sensitization and challenge. We did not assess AHR in the current study. This work extends knowledge of the role of STAT6 in allergic airway disease and is novel because it demonstrates that MWCNTs exacerbate components of HDM allergen-induced lung disease in WT mice (i.e., enhanced serum IgE, mucous cell metaplasia, airway fibrosis) through a STAT6-dependent mechanism.

A unique approach used in this study is the exposure method for delivering MWCNTs to the lungs of mice. To our knowledge, this is the first study that used intranasal aspiration exposure to deliver MWCNTs into the lungs of mice. This method is commonly used to deliver allergens to the pulmonary immune system and represents a more real-world exposure compared to oropharyngeal aspiration, which delivers a bolus dose of MWCNTs suspended in medium directly to the proximal trachea, bypassing the nasal cavity entirely. Though we did not histologically evaluate the nasal cavities in this study, it is likely that a large proportion of MWCNTs were retained in that region. The total intranasal MWCNT dose that mice received over 6 consecutive exposures was approximately 3 mg/kg, which is similar to a high dose (4 mg/kg) used previously in our studies (Duke et al., 2017; Sayers et al., 2013; Thompson et al., 2015). However histopathological evaluation clearly showed that the dose delivered to the lungs was much lower than that seen in our previous studies with oropharyngeal aspiration, where agglomerates of MWCNTs in lung tissue are clearly visible by light microscopy (Sayers et al., 2013; Thompson et al., 2015). In the present study, we did not observe extracellular agglomerates of MWCNTs in the lungs of either WT or *Stat6* KO mice after repeated intranasal aspiration. We did, however, observe small intracellular agglomerates and singlet MWCNTs within alveolar macrophages in lung tissue sections stained with hematoxylin and eosin (Fig. 1C), demonstrating that MWCNTs were delivered to professional phagocytes in the distal lung. The absence of lung inflammation with exposure to MWCNTs alone was likely due in part to this relatively low pulmonary dose.

While this study demonstrates that STAT6 plays a role in exacerbation of HDM allergen induced lung disease by MWCNTs, the underlying mechanism(s) through which MWCNTs

amplify the allergic response remains to be elucidated. It is possible that the strong adjuvant-like effects observed with co-exposure to MWCNTs and HDM could be due to heightened systemic inflammation, with elevated serum IgE, which then promotes greater lung inflammation upon further HDM exposure. Indeed, we observed a synergistic effect of MWCNTs and HDM on increasing serum IgE, where MWCNTs or HDM exposure alone did not significantly increase IgE levels above vehicle control (Fig. 4). The lack of increase in serum IgE by HDM alone is likely due to the relatively mild sensitization and challenge protocol used (Fig. 1), since we previously reported that a more robust treatment protocol using daily intranasal aspiration (5 days a week for two weeks) resulted in significantly elevated serum IgE (Shipkowski et al., 2015). The synergistic increase in serum IgE caused by MWCNTs and HDM suggests that MWCNTs amplify the adaptive immune response, which is required for synthesis of IgE by B cells.

Another intriguing potential mechanism for MWCNT exacerbation of allergic airway disease is the formation of an 'allergen corona' on the MWCNTs. The corona (or biocorona) refers to proteins, nucleic acids, or lipids, typically from the host, that adhere to the surface of the MWCNTs (Bhattacharya et al., 2016). Foreign biomolecules, including allergens, also bind to nanoparticles. For example, the proteolytic activities of several major allergens, birch pollen (Bet v 1), timothy grass pollen (Phl p 5) and house dust mite (Der p 1), were increased when bound to the surface of gold nanoparticles (Radauer-Preiml et al., 2016). We have recently discovered, using a proteomics approach, that a variety of proteins in HDM extract, including the allergen Der p 1, bind to MWCNTs to form an allergen corona (unpublished data). Through allergen corona formation, MWCNTs might increase the proteolytic activity of HDM allergens or facilitate delivery, uptake or presentation of allergens to immune cells.

We observed that WT mice, but not *Stat6* KO mice, had significant airway fibrosis, measured by morphometry of histopathology sections, after co-exposure to HDM and MWCNTs by intranasal aspiration, yet exposure to the MWCNTs or HDM alone did not significantly increase airway fibrosis (Fig. 5). The lack of lung fibrosis in WT mice exposed to MWCNTs in the present study is likely due to the relatively low dose achieved in the lungs using intranasal aspiration (discussed in detail above). The degree of lung fibrosis also could be due to the type of MWCNTs used in the present study. In experiments with mice using oropharyngeal aspiration exposure, the tangled MWCNTs used in the present study produced minimal lung fibrosis compared with with rod-like MWCNTs (Mitsui-7) (Duke et al., 2017). Other studies have shown that relatively high doses of the same MWCNTs used in the present study, by inhalation (30 mg/m$^3$, 6 hr) or by oropharyngeal aspiration (4 mg/kg), did not produce significant lung fibrosis in WT mice (Duke et al., 2017; Ryman-Rasmussen et al., 2009). Pulmonary fibrosis induced by the rod-like Mitsui-7 MWCNTs delivered by oropharyngeal aspiration was significantly reduced in *Stat6* KO mice (Nikota et al., 2017). However, it is important to note that Mitsui-7 are not typical of most commercially available types of MWCNTs, which are tangled rather than rod-like, and do not stimulate $T_H2$ type immune responses, including STAT6 activation, in the absence of allergen exposure (Shipkowksi et al., 2015; Duke et al., 2017; Ihrie et al., 2019). In another study, *Stat6* KO mice also display reduced airway fibrosis in response to *Alternaria*, a fungal

allergen (Doherty et al., 2012a, 2012b). Collectively, these investigations show that STAT6 plays an important role in pulmonary fibrogenesis induced by allergens and nanoparticles.

We detected few significant changes in pro-fibrotic cytokines in BALF after exposure to HDM, MWCNTs or the combination of HDM and MWCNTs (Fig. 6). IL-13 was suppressed by MWCNTs in the absence or presence of HDM extract in WT mice, but not *Stat6* KO mice. IL-13 is typically induced by allergen exposure in the lungs of mice, so it is possible that this $T_H2$ cytokine was induced earlier and returned to a baseline level (or below) the time of necropsy. IL-1β in BALF was constitutively lower in *Stat6* KO compared to WT but was induced in *Stat6* KO mice by HDM extract. We previously reported that IL-1β production, mediated through inflammasome activation, was increased in the lungs of mice 21 days after oropharyngeal aspiration of MWCNTs (Shipkowski et al., 2015). The lack of induction of IL-1β by MWCNTs in the present study, or other pro-fibrotic cytokines (TGF-β1 and OPN) could be due to the relatively low dose of MWCNTs delivered to the lungs by intranasal aspiration.

There is abundant evidence that STAT6 promotes allergic lung disease (Walford and Doherty, 2013), and our work show that STAT6 also contributes to exacerbation of allergic lung disease by MWCNTs. Other STAT family members also play important regulatory roles in allergic lung disease. For example, STAT3 enhances the actions of TGF-β1 through crosstalk with Smad3 to promote fibroblast to myofibroblast differentiation, thereby contributing to fibrosis (Pedroza et al., 2018). STAT3 and STAT6 are phosphorylated by canonical cytokines binding to their cognate receptors; IL-6 or PDGF binding activates STAT3, while IL-4 or IL-13 activates STAT6 (Bonner, 2010). Our Western blotting data showed that co-exposure of WT mice to HDM and MWCNT by intranasal aspiration induced a significant increase in the phosphorylation of STAT3, whereas HDM or MWCNTs alone did not increase STAT3 phosphorylation (Fig. 7). Moreover, STAT3 phosphorylation in *Stat6* KO mice was also increased by co-exposure to HDM and MWCNTs, albeit not significantly, and was not significantly different from WT mice co-exposed to HDM and MWCNTs. In contrast to STAT3, which could complement the actions of STAT6 in promoting allergic airway inflammation, STAT1 is involved in $T_H1$ immune responses and opposes the $T_H2$ immune responses mediated via STAT6 (Bonner, 2010). For example, we previously reported that *Stat1* KO mice are susceptible to OVA-induced lung inflammation and exacerbation of OVA-induced airway fibrosis by MWCNTs (Thompson et al., 2015). In the present study, we did not detect the phosphorylation of STAT1 in lung tissue from either WT or *Stat6* KO mice. However, our previous work with *Stat1* KO mice clearly shows that STAT1 plays a protective role in the exacerbation of allergic airway disease by MWCNTs, while the current work shows that STAT6 promotes the exacerbation of allergic airway disease by MWCNTs. Therefore, STAT1 and STAT6 play opposing roles in the exacerbation of allergic lung disease in mice by MWCNTs.

## 5. Conclusions

The findings presented in this report support a role for STAT6 in the exacerbation of HDM-induced allergic airway disease in mice by MWCNTs. *Stat6* KO mice were protected from allergic airway disease induced by co-exposure to HDM and MWCNTs. The role of STAT6

in promoting the exacerbation of allergen-induced lung disease in mice is in direct opposition to the role of STAT1, since our previous work showed that *Stat1* KO mice were susceptible to allergic airway disease induced by co-exposure to HDM and MWCNTs. Therefore, the balance between STAT6 and STAT1 signaling is likely important in determining the severity of exacerbations caused by nanoparticle exposure in individuals with asthma.

## Acknowledgements

## Abbreviations:

| | |
|---|---|
| **MWCNT** | multiwalled carbon nanotube |
| **HDM** | house dust mite |
| **STAT6** | Signal transducer and activator of transcription 6 |
| **ENM** | engineered nanomaterial |

## References

Akimoto T, Numata F, Tamura M, Takata Y, Higashida N, Takashi T, Takeda K, Akira S, 1998. Abrogation of bronchial eosinophilic inflammation and airway hyperreactivity in signal transducers and activators of transcription (STAT)6-deficient mice. J. Exp. Med 187, 1537–42. [PubMed: 9565645]

Bhattacharya K, Mukherjee SP, Gallud A, Burkert SC, Bistarelli S, Bellucci S, Bottini M, Star A, Fadeel B, 2016. Biological interactions of carbon-based nanomaterials: From coronation to degradation. Nanomedicine Nanotechnology, Biol. Med 10.1016/j.nano.2015.11.011

Bonner JC, 2010. Mesenchymal cell survival in airway and interstitial pulmonary fibrosis. Fibrogenes. tissue repair 10.1186/1755-1536-3-15

Castañeda AR, Pinkerton KE, 2016. Investigating the Effects of Particulate Matter on House Dust Mite and Ovalbumin Allergic Airway Inflammation in Mice . Curr. Protoc. Toxicol 68, 18.18.1–18.18.18. 10.1002/cptx.5 [PubMed: 27145110]

Chapoval SP, Dasgupta P, Smith EP, DeTolla LJ, Lipsky MM, Kelly-Welch AE, Keegan AD, 2011. STAT6 expression in multiple cell types mediates the cooperative development of allergic airway disease. J. Immunol 186, 2571–83. 10.4049/jimmunol.1002567 [PubMed: 21242523]

Doherty TA, Khorram N, Chang JE, Kim H-K, Rosenthal P, Croft M, Broide DH, 2012a. STAT6 regulates natural helper cell proliferation during lung inflammation initiated by Alternaria. Am. J. Physiol. Lung Cell. Mol. Physiol 303, L577–88. 10.1152/ajplung.00174.2012 [PubMed: 22865552]

Doherty TA, Khorram N, Sugimoto K, Sheppard D, Rosenthal P, Cho JY, Pham A, Miller M, Croft M, Broide DH, 2012b. Alternaria induces STAT6-dependent acute airway eosinophilia and epithelial FIZZ1 expression that promotes airway fibrosis and epithelial thickness. J. Immunol 188, 2622–9. 10.4049/jimmunoL.l101632 [PubMed: 22327070]

Donaldson K, Aitken R, Tran L, Stone V, Duffin R, Forrest G, Alexander A, 2006. Carbon Nanotubes: A Review of Their Properties in Relation to Pulmonary Toxicology and Workplace Safety. Toxicol. Sci 92, 5–22. 10.1093/toxsci/kfjl30 [PubMed: 16484287]

Duke KS, Bonner JC, 2018. Mechanisms of carbon nanotube-induced pulmonary fibrosis: a physicochemical characteristic perspective. WIREs Nanomedicine and Nanobiotechnology 10, e1498. 10.1002/wnan.1498 [PubMed: 28984415]

Duke KS, Taylor-Just AJ, Ihrie MD, Shipkowski KA, Thompson EA, Dandley EC, Parsons GN, Bonner JC, 2017. STAT1-dependent and -independent pulmonary allergic and fibrogenic responses in mice after exposure to tangled versus rod-like multi-walled carbon nanotubes. Part. Fibre Toxicol 14, 26. 10.1186/s12989-017-0207-3 [PubMed: 28716119]

Hebenstreit D, Wirnsberger G, Horejs-Hoeck J, Duschl A, 2006. Signaling mechanisms, interaction partners, and target genes of STAT6 . Cytokine Growth Factor Rev . 10.1016/j.cytogfr.2006.01.004

Holgate ST, 2009. Pathogenesis of Asthma, in: Allergy and Allergic Diseases. Wiley-Blackwell, Oxford, UK, pp. 1608–1631. 10.1002/9781444300918.ch78

Ihrie MD, Bonner JC, 2018. The Toxicology of Engineered Nanomaterials in Asthma. Curr. Environ. Heal. Reports 5, 100–109. 10.1007/s40572-018-0181-4

Ihrie MD, Taylor-Just AJ, Walker NJ, Stout MD, Gupta A, Richey JS, Hayden BK, Baker GL, Sparrow BR, Duke KS, Bonner JC, 2019. Inhalation exposure to multi-walled carbon nanotubes alters the pulmonary allergic response of mice to house dust mite allergen. Inhal. Toxicol 31, 192–202. 10.1080/08958378.2019.1643955 [PubMed: 31345048]

Inoue K, Koike E, Yanagisawa R, Hirano S, Nishikawa M, Takano H, 2009. Effects of multi-walled carbon nanotubes on a murine allergic airway inflammation model. Toxicol. Appl. Pharmacol . 10.1016/j.taap.2009.04.003

Kim HY, DeKruyff RH, Umetsu DT, 2010. The many paths to asthma: phenotype shaped by innate and adaptive immunity. Nat. Immunol 11, 577–84. 10.1038/ni.1892 [PubMed: 20562844]

Kuperman D, Schofield B, Wills-Karp M, Grusby MJ, 1998. Signal transducer and activator of transcription factor 6 (Stat6)-deficient mice are protected from antigen-induced airway hyperresponsiveness and mucus production. J. Exp. Med 187, 939–48. [PubMed: 9500796]

Nikota J, Banville A, Goodwin LR, Wu D, Williams A, Yauk CL, Wallin H, Vogel U, Halappanavar S, 2017. Stat-6 signaling pathway and not Interleukin-1 mediates multi-walled carbon nanotube-induced lung fibrosis in mice: insights from an adverse outcome pathway framework. Part. Fibre Toxicol 14, 37. 10.1186/s12989-017-0218-0 [PubMed: 28903780]

Nygaard UC, Hansen JS, Samuelsen M, Alberg T, Marioara CD, Løvik M, 2009. Single-Walled and Multi-Walled Carbon Nanotubes Promote Allergic Immune Responses in Mice . Toxicol. Sci . 10.1093/toxsci/kfp057

Ozdoganoglu T, Songu M, 2012. The burden of allergic rhinitis and asthma. Ther. Adv. Respir. Dis 6, 11–23. 10.1177/1753465811431975 [PubMed: 22179899]

Pedroza M, To S, Assassi S, Wu M, Tweardy D, Agarwal SK, 2018. Role of STAT3 in skin fibrosis and transforming growth factor beta signalling . Rheumatol. (Oxford, England) 10.1093/rheumatology/kex347

Radauer-Preiml I, Andosch A, Hawranek T, Luetz-Meindl U, Wiederstein M, Horejs-Hoeck J, Himly M, Boyles M, Duschl A, 2016. Nanoparticle-allergen interactions mediate human allergic responses: protein corona characterization and cellular responses. Part. Fibre Toxicol 10.1186/sl2989-016-0113-0

Rawlings JS, Rosler KM, Harrison D. a, 2004. The JAK/STAT signaling pathway. J. Cell Sci 117, 1281–1283. 10.1242/jcs.00963 [PubMed: 15020666]

Ronzani C, Casset A, Pons F, 2014. Exposure to multi-walled carbon nanotubes results in aggravation of airway inflammation and remodeling and in increased production of epithelium-derived innate cytokines in a mouse model of asthma. Arch. Toxicol 88, 489–499. 10.1007/s00204-013-1116-3 [PubMed: 23948970]

Rydman EM, Ilves M, Koivisto AJ, Kinaret PAS, Fortino V, Savinko TS, Lehto MT, Pulkkinen V, Vippola M, Hämeri KJ, Matikainen S, Wolff H, Savolainen KM, Greco D, Alenius H, 2014. Inhalation of rod-like carbon nanotubes causes unconventional allergic airway inflammation. Part. Fibre Toxicol 11, 48. 10.1186/sl2989-014-0048-2 [PubMed: 25318534]

Ryman-Rasmussen, Jessica P, Cesta MF, Brody AR, Shipley-Phillips JK, Everitt JI, Tewksbury EW, Moss OR, Wong BA, Dodd DE, Andersen ME, Bonner JC, 2009. Inhaled carbon nanotubes reach the subpleural tissue in mice . Nat. Nanotechnol . 10.1038/nnano.2009.305

Ryman-Rasmussen Jessica P., Tewksbury EW, Moss OR, Cesta MF, Wong B. a., Bonner JC, 2009. Inhaled multiwalled carbon nanotubes potentiate airway fibrosis in murine allergic asthma. Am. J. Respir. Cell Mol. Biol 40, 349–358. 10.1165/rcmb.2008-02760C [PubMed: 18787175]

Sayers BC, Taylor AJ, Glista-Baker EE, Shipley-Phillips JK, Dackor RT, Edin ML, Lih FB, Tomer KB, Zeldin DC, Langenbach R, Bonner JC, 2013. Role of cyclooxygenase-2 in exacerbation of allergen-induced airway remodeling by multiwalled carbon nanotubes . Am. J. Respir. cell Mol. Biol . 10.l165/rcmb.2013-00190C

Shipkowski KA, Taylor AJ, Thompson EA, Glista-Baker EE, Sayers BC, Messenger ZJ, Bauer RN, Jaspers I, Bonner JC, 2015. An Allergic Lung Microenvironment Suppresses Carbon Nanotube-Induced Inflammasome Activation via STAT6-Dependent Inhibition of Caspase-1. PLoS One 10, e0128888–e0128888. 10.1371/journal.pone.0128888 [PubMed: 26091108]

Taylor AJ, McClure CD, Shipkowski KA, Thompson EA, Hussain S, Garantziotis S, Parsons GN, Bonner JC 2014. Atomic layer deposition coating of carbon nanotubes with aluminum oxide alters pro-fibrogenic cytokine expression by human mononuclear phagocytes in vitro and reduces lung fibrosis in mice in vivo. PLoS One. 9(9): el06870. 10.1371/journal.pone.0106870

Thompson EA, Sayers BC, Glista-Baker EE, Shipkowski KA, Ihrie MD, Duke KS, Taylor AJ, Bonner JC 2015. Role of Signal Transducer and Activator of Transcription 1 in Murine Allergen—Induced Airway Remodeling and Exacerbation by Carbon Nanotubes. Am. J. Respir. Cell Mol. Biol 53, 625–636.10.1165/rcmb.2014-0221OC [PubMed: 25807359]

Walford HH, Doherty TA 2013. STAT6 and lung inflammation. Jak-Stat 2, e25301. 10.4161/jkst.25301 [PubMed: 24416647]

WHO Environmental Health Criteria Document 244: Principles and methods to assess the risk of immunotoxicity associated with exposure to nanomaterials. Geneva: World Health Organization, International Programme on Chemical Safety. 2020, 380 pgs.

Author Manuscript

Author Manuscript

Author Manuscript

Author Manuscript

**Highlights**

- The role of the transcription factor STAT6 in exacerbation of allergen-induced lung disease by multi-walled carbon nanotubes delivered via intranasal aspiration was investigated using wild type C57BL/6 and *Stat6* knockout mice.

- Multi-walled carbon nanotubes exacerbated house dust mite allergen-induced eosinophilic lung inflammation, mucous cell metaplasia and serum IgE in wild type mice, and these allergic endpoints were ablated in *Stat6* knockout mice.

- Airway fibrosis was increased by co-exposure to house dust mite allergen and multi-walled carbon nanotubes in wild type mice, but not in *Stat6* knockout mice.

- Theses findings are the first to demonstrate that exacerbation of allergic lung disease by carbon nanotubes is STAT6-dependent.
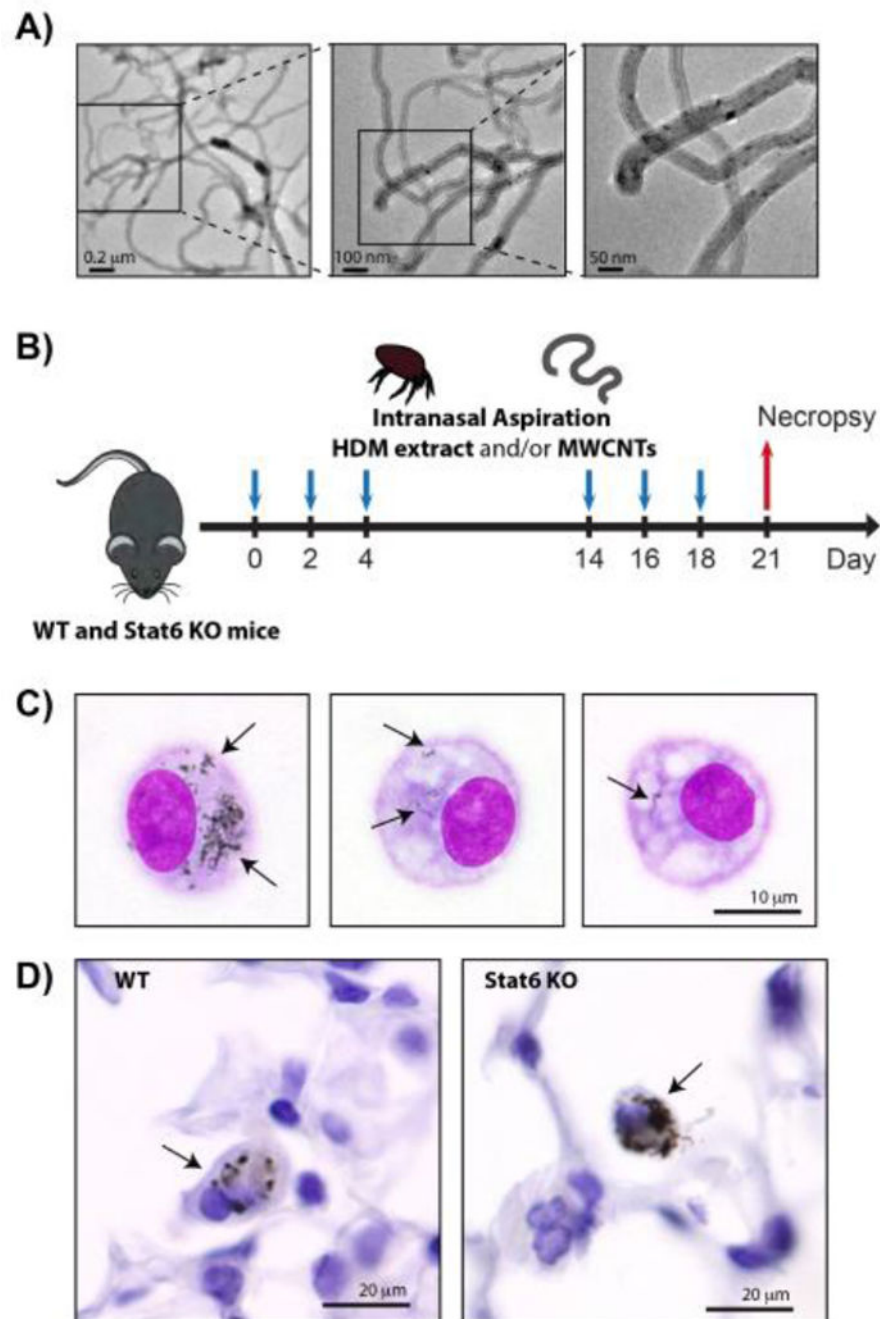
**Figure 1.**
**A)** TEM images of the MWCNTs used in this study. **B)** Illustration of exposure protocol timeline. Wild type (WT) and *Stat6*<sup>−/−</sup> mice were exposed repeatedly to HDM extract and/or MWCNTs by intranasal aspiration at days 0, 2 and 4, followed another round of repeated intranasal aspiration exposure at days 14, 16 and 18. Necropsy was performed at day 21 to collect BALF, lung tissue and serum. See the Methods section for details. **C)** Oil immersion (1000x) images of alveolar macrophages isolated by Cytospin centrifugation from the BALF of WT mice 21 days after exposure to MWCNTs using the protocol illustrated in panel B.

Arrows indicate MWCNTs in the cytoplasm. **D)** Oil immersion (1000x) images of MWCNTs in the lung tissue of WT and Stat6 mice *in situ*. Arrows indicate macrophages with MWCNT inclusions.
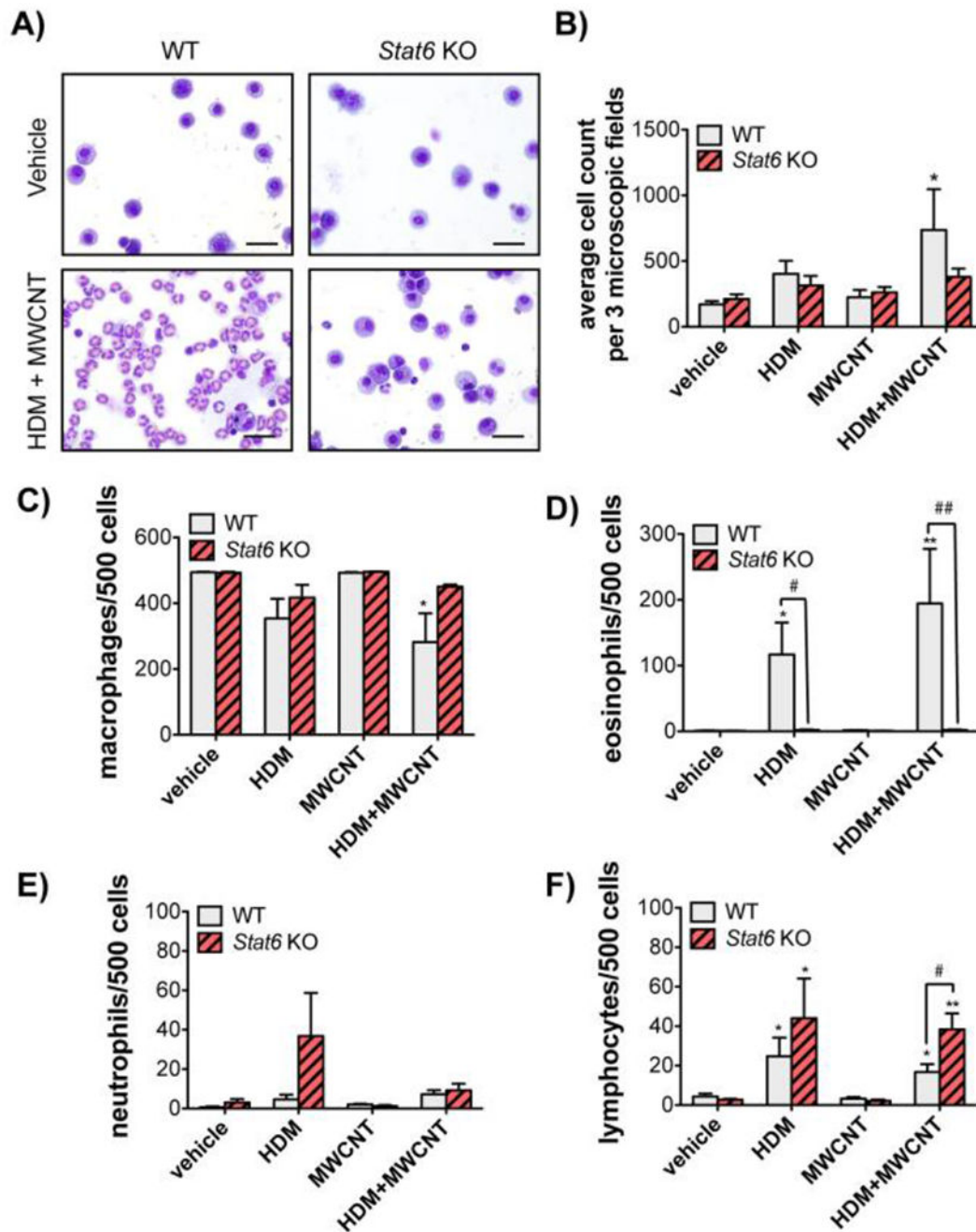
**Figure 2. Analysis of inflammatory cells in the BALF of WT and *Stat6* KO mice after exposure to MWCNTs with or without HDM allergen.**

**A)** Representative photomicrographs of BALF cells isolated by Cytospin centrifugation from WT and *Stat6* KO mice after exposure to vehicle or HDM extract and MWCNTs (Bars = 20 μm). **B)** Total cell counts from Cytospin slides in each treatment group from WT and *Stat6* KO mice. Three microscopic frames per slide were counted at 100x magnification for each animal. *p<0.05 vs. vehicle, Mann-Whitney test. **C)** Numbers of macrophages per 500 cells in the BALF of animals from each treatment group. *p<0.05 vs. vehicle of same genotype.

**D)** Numbers of eosinophils per 500 cells. *p<0.05 or **p<0.01 compared to vehicle in WT mice. #p<0.05 or ##p<0.01 between genotypes. One-way ANOVA. **E)** Numbers of neutrophils per 500 cells. **F)** Numbers of lymphocytes per 500 cells. *p<0.05 or **p<0.01 vs. vehicle of same genotype. #p<0.05 between genotypes, one-way ANOVA. N=4 to 6 animals per group for panels **B-F.**

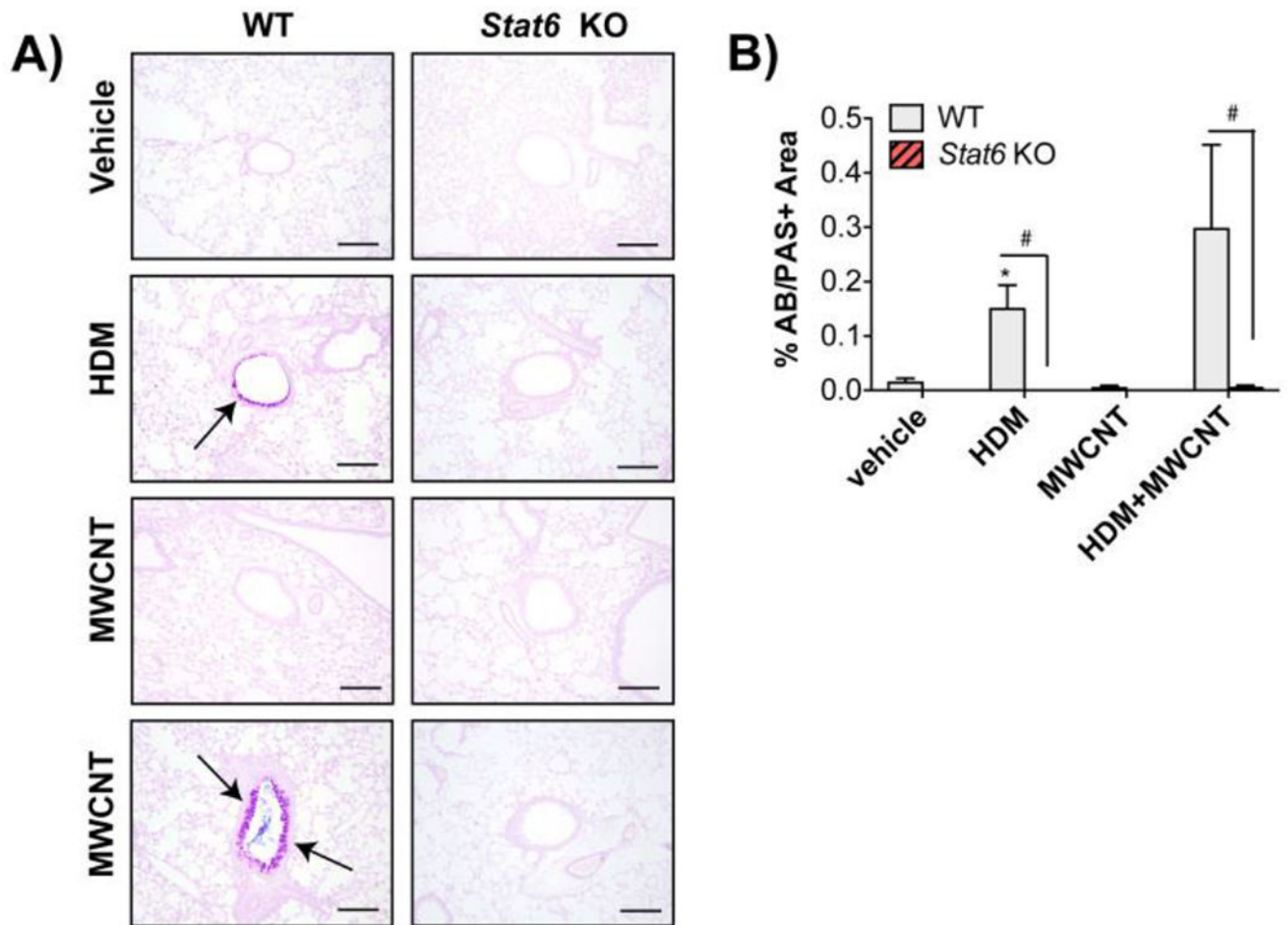**Figure 3. Requirement of STAT6 for HDM-induced mucous cell metaplasia and exacerbation by MWCNTs in mice.**

**A)** Representative photomicrographs of Alcian blue periodic acid Schiff (AB/PAS) stained lung sections in WT and *Stat6*KO mice after exposure to vehicle, HDM, MWCNTs or MWCNTs with HDM allergen (Bars = 200 μm). **B)** Quantification of AB/PAS-positive mucosubstances in the airways of WT and *Stat6* KO mice. N=4 to 6 animals per group. *p<0.05 vs. vehicle of same genotype, Student's t-test. #p< 0.05 between WT and *Stat6* KO mice, Mann-Whitney test.
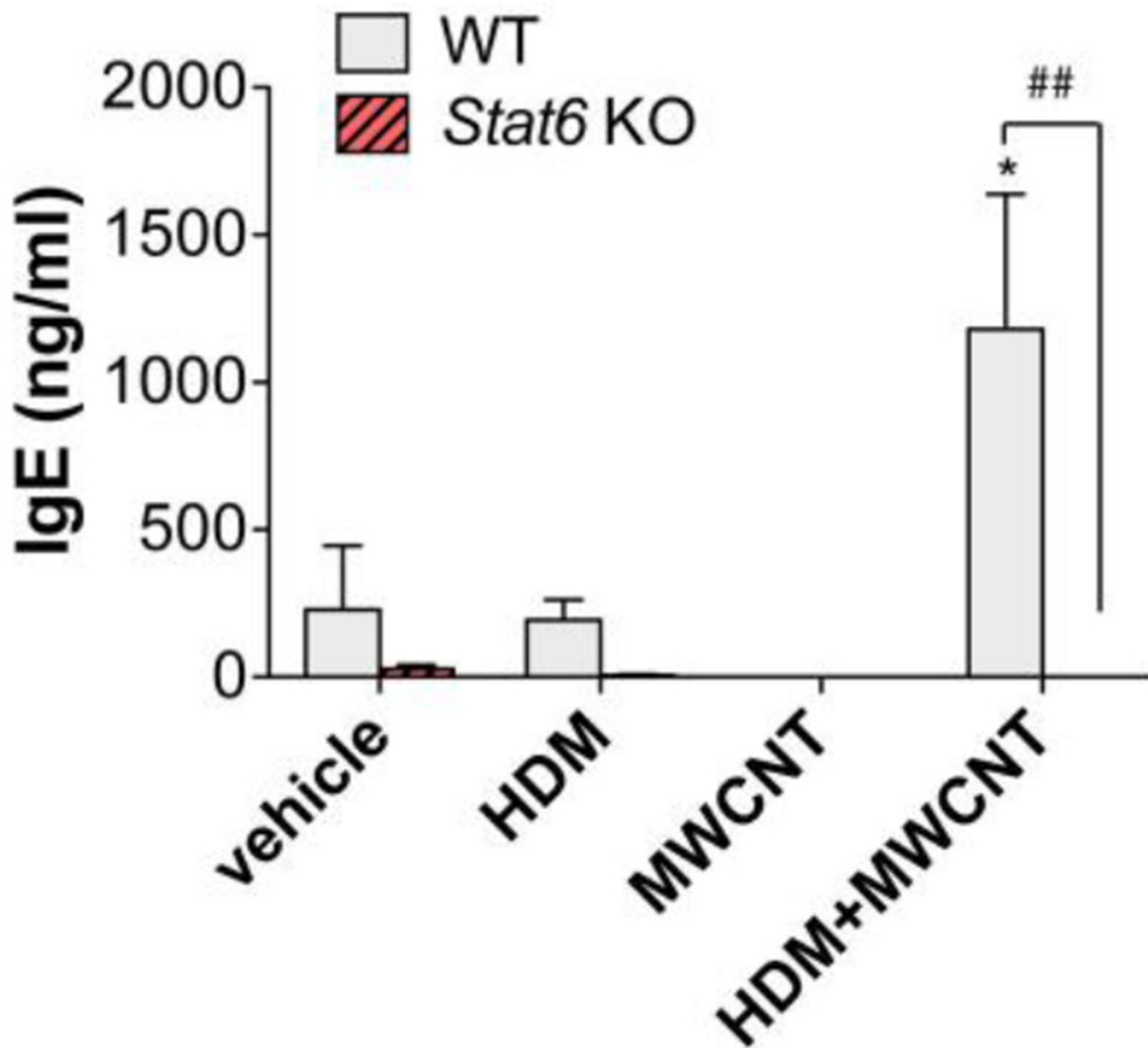
**Figure 4. Serum IgE is increased by combined HDM and MWCNT exposure in the lungs of WT mice but not in *Stat6* KO mice.**

Blood was collected from mice at necropsy and serum IgE was measured by ELISA. N=4 to 6 animals per group. *p<0.05 vs. vehicle of same genotype, ##p< 0.01 between WT and *Stat6* KO mice, one-way ANOVA.
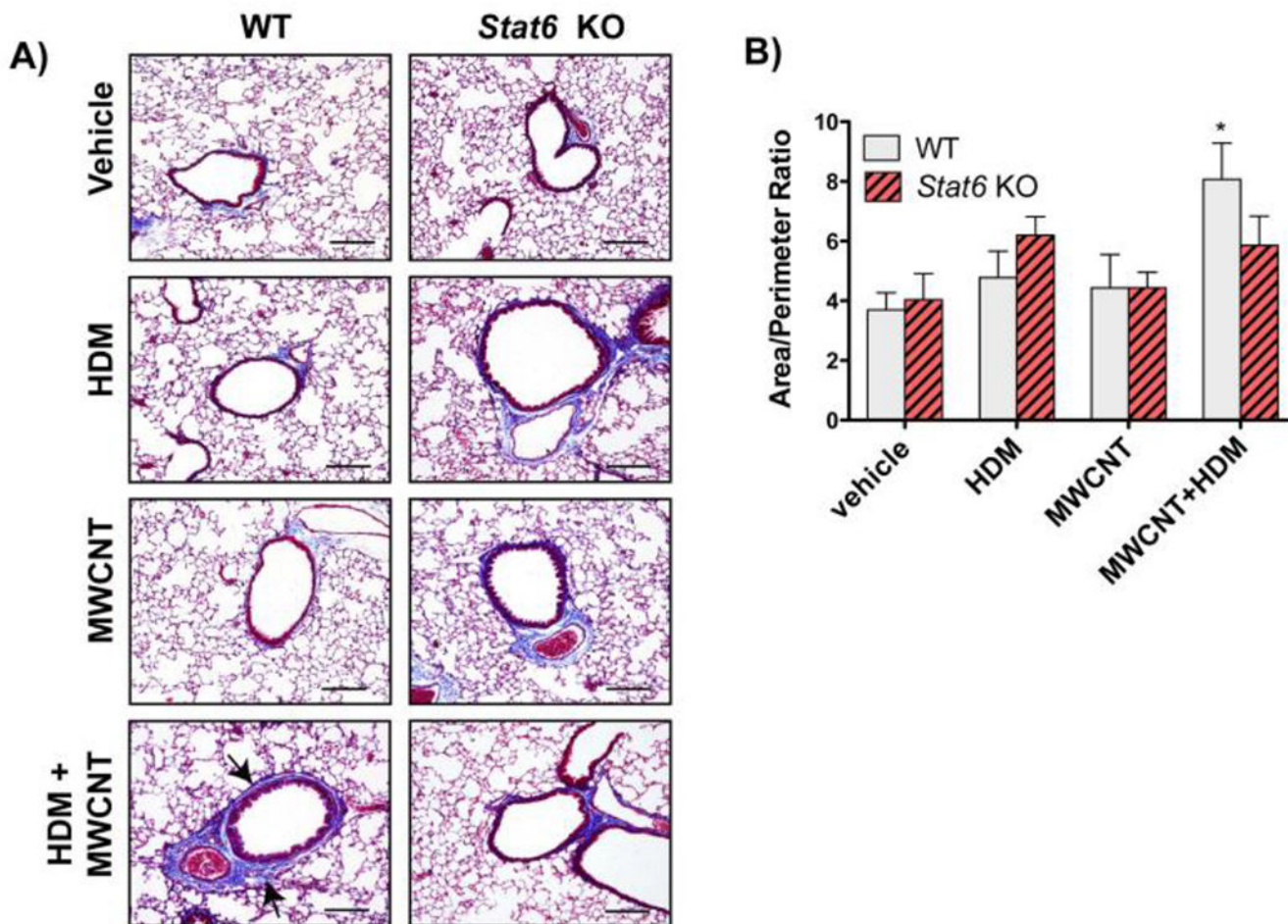
**Figure 5. Airway fibrosis is increased by combined HDM and MWCNT exposure in the lungs of WT mice but not in *Stat6* KO mice.**

**A)** Representative photomicroscopic images of Gomori's trichrome-stained lung sections from animals in each of the treatment groups in each genotype (Bars = 200 μm). **B)** Area to perimeter analysis of trichrome stained lung sections showed a significant increase in airway fibrosis caused by the combination of MWCNTs and HDM extract in WT mice. N=4 to 6 animals per group for each genotype. *$p < 0.05$ vs. vehicle, one-way ANOVA.
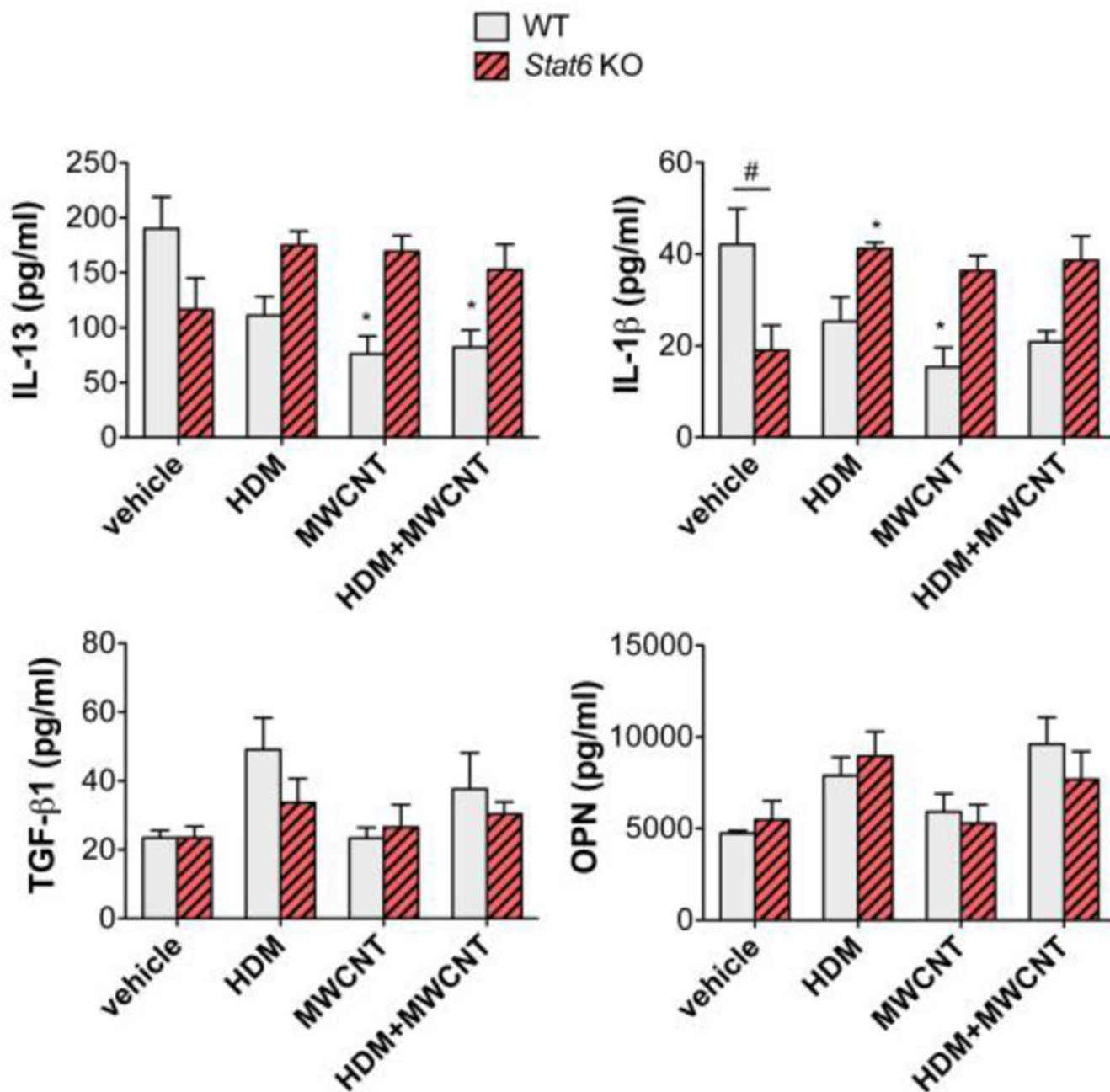
**Figure 6. Cytokine levels in the BALF of WT and *Stat6* KO mice after exposure to HDM extract in the absence or presence of MWCNTs.**

BALF was collected from mice at necropsy. Cytokines in BALF (IL-13, IL-1β, TGF-β1, OPN) were measured by ELISA as described in the Methods section. N=4 to 6 animals per group. *p<0.05 vs. vehicle of same genotype, #p< 0.05 between WT and *Stat6* KO mice, one-way ANOVA.
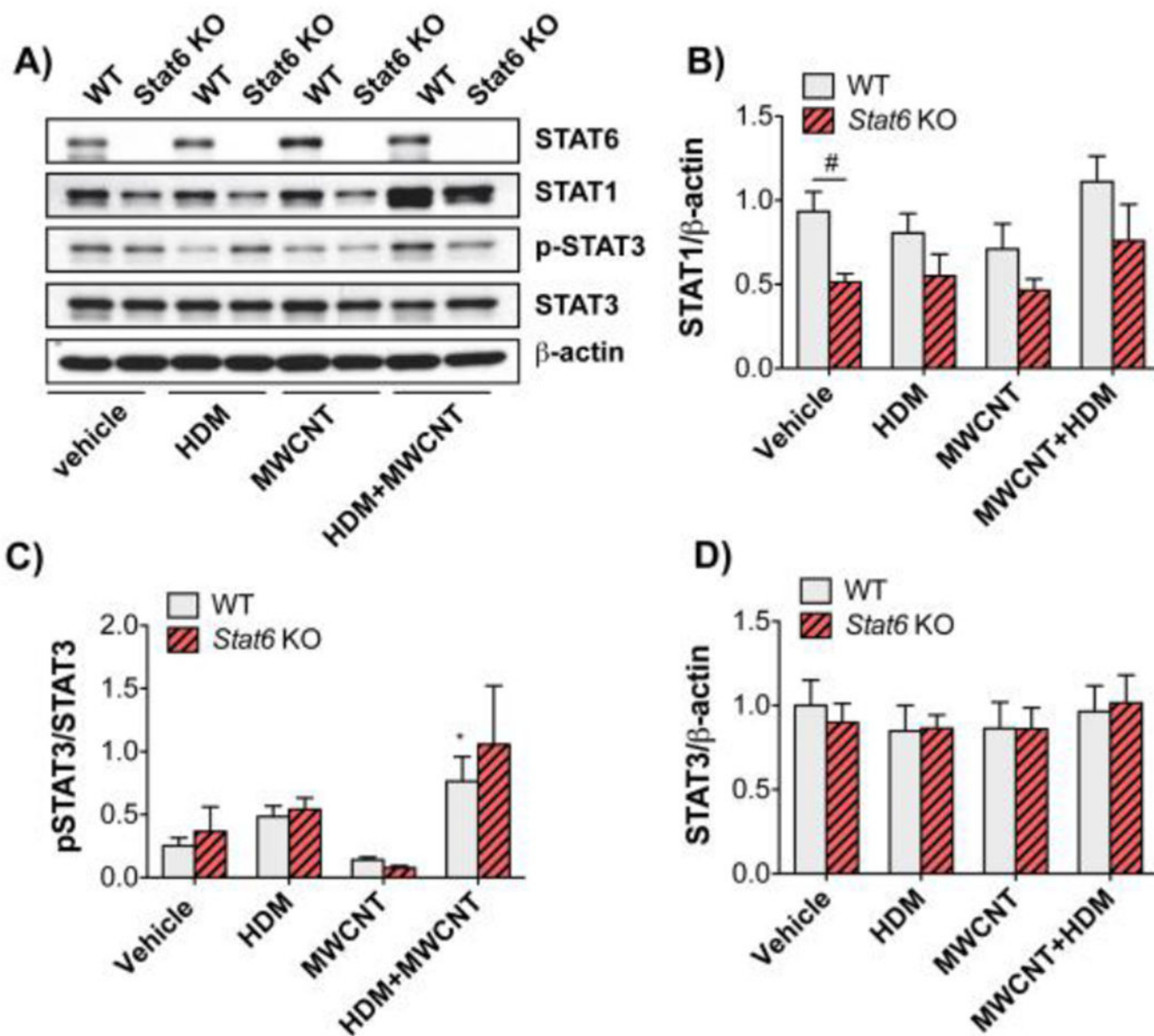
**Figure 7. STAT protein levels and activation in lung tissue from WT and *Stat6* KO mice after treatment with HDM extract in the absence or presence of MWCNTs.**

Protein lysates of right lung lobe tissue collected from mice at necropsy were assayed by Western blotting for STAT proteins and β-actin. **A)** Representative Western blots of lung tissue from WT or *Stcit6* KO mice exposed to vehicle, HDM, MWCNTs, or HDM and MWCNTs. **B)** Densitometry of STAT1 signal normalized against the β-actin signal. #P < 0.05 between genotypes, one-way ANOVA. N=5 animals per group. **C)** Densitometry of p-STAT3 normalized against total STAT3. *P < 0.05 compared to vehicle, Mann-Whitney test. **D)** Densitometry of total STAT3 normalized against β-actin. N=4 to 6 animals per group.